Synthesis of Tubular Gold and Silver Nanoshells Using Silica Nanowire Core Templates

Yongquan Qu, Rhiannon Porter, Fang Shan, Joshua D. Carter, and Ting Guo*

Department of Chemistry, University of California, Davis, California 95616

Received February 6, 2006. In Final Form: April 5, 2006

We report the synthesis of tubular gold and silver nanoshells on silica nanowire core templates in solution. Silica nanowires were synthesized and characterized with optical and NMR methods. Gold nanoparticle seeds (2 to 3 nm) with weak repulsive surfactants such as tetrakis-hydroxymethyl-phosphonium chloride (THPC) were conjugated to the surface of these nanowires. A regrowth process was initiated from these nanoparticles on the surface of the silica nanowires dispersed in gold or silver stock solutions in the presence of reducing agents. Micrometers-long gold and silver tubular nanoshells (80−150 nm o.d.) were made, fully covering the silica nanowires.

Introduction

Nanomaterials with the most easily modified surface are desirable as templates. Silica presents itself as an excellent candidate. Although making metal tubular nanoshells from silica nanowire core templates is a novelty to be discussed here, work related to using silica materials as templates dates back to early investigations of nanoparticles deposited on chemically treated *flat* surfaces of materials such as silicon wafers and patterning nanoparticles on flat surfaces. [1−4] Those efforts have yielded important basic knowledge that has become a foundation for much of the current work of making composite nanostructures. Recently, various nanoparticles have been attached to silica beads/nanoparticles, and gold nanoshells have been made on the surface of silica beads/nanoparticles.[5−7] In another work, silica nanorods (very short wires) have been used as templates to make silver nanotubes.[8] Here we will explore for the first time using silica nanowires (SiNWs) as templates to make gold or silver tubular nanoshells (or nanotubes).

SiNWs themselves have been extensively studied, and silicon and silica nanowires (both denoted as SiNWs here) have been made by many groups.[9−13] For example, SiNWs can be made in solution under supercritical conditions.[14] Laser vaporization and CVD methods have also been employed to produce SiNWs.[15,16] An extrusion method has been developed to make coaxial nanowires.[17] The diameter of these SiNWs ranges from 3 to 500 nm, and the length ranges from a few micrometers to millimeters. Because most silicon nanowires have a thin oxide layer on the surface, both silicon and silica nanowires are good candidates for templates.

These nanowire templates can be used as backbones in future nanoscale devices. For example, one-dimensional nanowires decorated with zero dimensional nanoparticles have been attempted in many applications such as sensors, solar cell panels, actuators, and catalysts.[18−21] As a result, nanowires with desirable template properties may become popular components in future nanoscale devices. To date, many prototypes such as nanorods and carbon nanotubes and biological molecules such as DNA have been used as backbone templates to make these complex three-dimensional nanostructures.[22−26] For instance, the direct deposition of metal onto nanowires/nanotubes has been reported in which no chemical modifications are employed before sputtering or decorating.[27] However, chemically modified carbon nanotubes have also been studied and proposed for various applications. For example, carbon nanotubes decorated with DNA have been used as sensors.[20,28−30] In addition, various materials such as dye molecules and DNA have been covalently linked to

* Corresponding author. E-mail: tguo@ucdavis.edu. Tel: (530) 754-5283. Fax: (530) 752-8995.

(1) Wang, M.; Liechti, K.; Wang, Q.; White, J. *Langmuir* **2005**, *21*, 1848−1857.
(2) Tien, J.; Terfort, A.; Whitesides, G. M. *Langmuir* **1997**, *13*, 5349−5355.
(3) Bae, S.; Lim, D.; Park, J.; Lee, W.; Cheon, J.; Kim, S. *J. Phys. Chem. B* **2004**, *108*, 2575−2579.
(4) Harada, Y.; Girolami, G.; Nuzzo, R. *Langmuir* **2004**, *20*, 10878−10888.
(5) Loo, C.; Lowery, A.; Halas, N.; West, J.; Drezek, R. *Nano Lett.* **2005**, *5*, 709−711.
(6) Tan, Y.; Ding, S.; Wang, Y.; Qian, W. *Acta Chim. Sin.* **2005**, *63*, 929−933.
(7) Osterloh, F.; Hiramatsu, H.; Porter, R.; Guo, T. *Langmuir* **2004**, *20*, 5553−5558.
(8) Park, J.; Oh, S.; Jo, B. *Mater. Chem. Phys.* **2004**, *87*, 301−310.
(9) Pan, Z.; Dai, Z.; Ma, C.; Wang, Z. *J. Am. Chem. Soc.* **2002**, *124*, 1817−1822.
(10) Tong, L.; Lou, J.; Ye, Z.; Svacha, G.; Mazur, E. *Nanotechnology* **2005**, *16*, 1445−1448.
(11) Zhang, H. F.; Wang, C. M.; Buck, E. C.; Wang, L. S. *Nano Lett.* **2003**, *3*, 577−580.
(12) Kameoka, J.; Verbridge, S.; Liu, H.; Czaplewski, D.; Craighead, H. *Nano Lett.* **2004**, *4*), 2105−2108.
(13) Gole, J.; Wang, Z.; Dai, Z.; Stout, J.; White, M. *Colloid Polym. Sci.* **2003**, *281*, 673−685.
(14) Holmes, J. D.; Johnston, K. P.; Doty, R. C.; Korgel, B. A. *Science* **2000**, *287*, 1471−1473.
(15) Morales, A. M.; Lieber, C. M. *Science* **1998**, *279*, 208−211.
(16) Wu, Y.; Cui, Y.; Huynh, L.; Barrelet, C.; Bell, D.; Lieber, C. *Nano Lett.* **2004**, *4*, 433−436.
(17) Xiong, Y.; Mayers, B.; Xia, Y. *Chem. Commun.* **2005**, 5013−5022.
(18) Lesniak, W.; Bielinska, A.; Sun, K.; Janczak, K.; Shi, X.; Baker, J.; Balogh, L. *Nano Lett.* **2005**, *5*, 2123−2130.
(19) Wu, Y.; Xiang, J.; Yang, C.; Lu, W.; Lieber, C. *Nature* **2004**, *430*, 61−65.
(20) Zhao, Q.; Nardelli, M.; Lu, W.; Bernholc, J. *Nano Lett.* **2005**, *5*, 847−851.
(21) Le, J.; Pinto, Y.; Seeman, N.; Musier-Forsyth, K.; Taton, T.; Kiehl, R. *Nano Lett.* **2004**, *4*, 2343−2347.
(22) Hochbaum, A.; Fan, R.; He, R.; Yang, P. *Nano Lett.* **2005**, *5*, 457−460.
(23) Lu, W.; Xiang, J.; Timko, B.; Wu, Y.; Lieber, C. *Proc. Natl. Acad. Sci. U.S.A.* **2005**, *102*, 10046−10051.
(24) Kanaras, A.; Sonnichsen, C.; Liu, H.; Alivisatos, A. *Nano Lett.* **2005**, *5*, 2164−2167.
(25) Sandstrom, P.; Boncheva, M.; Akerman, B. *Langmuir* **2003**, *19*, 7537−7543.
(26) Shenhar, R.; Rotello, V. M. *Acc. Chem. Res.* **2003**, *36*, 549−561.
(27) Cassell, A. M.; Raymakers, J. A.; Kong, J.; Dai, H. J. *J. Phys. Chem. B* **1999**, *103*, 6484−6492.
(28) Staii, C.; Johnson, A. *Nano Lett.* **2005**, *5*, 1774−1778.
(29) Heller, D.; Jeng, E.; Yeung, T.; Martinez, B.; Moll, A.; Gastala, J.; Strano, M. *Science* **2006**, *311*, 508−511.
(30) Zeng, L.; Zhang, L.; Barron, A. *Nano Lett.* **2005**, *5*, 2001−2004.

10.1021/la060359m CCC: $33.50
Published on Web 06/06/2006 PAGE EST: 8

ZnO or gold nanowires.[31,32] These results have proven that it is possible to use chemical means to modify nanowires and nanotubes, and such modifications will lend further control to the eventual functions of these complicated nanostructures. In addition, the applications of silica nanowires themselves have been explored by many groups because they can be used as components in future nanoscale electronics and light emitters,[33−37] and gold has been vacuum plated onto SiNWs to make gold nanoparticles.[38,39]

We have developed a new method to make SiNWs in bulk quantities (>100 mg). We will present results on the bulk synthesis, characterization, and manipulation of these SiNWs. These results show that these nanowires possess superior properties as templates. All of the templating reactions were carried out in solution, and gold and silver tubular nanoshells were successfully made for the first time using chemical modification of the silica surface and regrowth processes in solution. These new materials represent a new brand of nanomaterials that may be widely used in future nanodevices as conductors, enhanced radiation absorbers, and even optical waveguides.

Materials and Methods

All chemicals were purchased from Aldrich and used without further treatment. Co nanoparticles were used for the catalytic growth of SiNWs. These nanoparticles were made via a high-temperature thermal decomposition method from $Co_2(CO)_8$ in a mixture of oleic acid (OA), trioctylphosphine oxide (TOPO), and trioctylamine (TOA) dissolved in dichlorobenzene (DCB).[40,41] Depending on the relative amounts of these surfactants in the mixture, Co nanoparticles of different sizes were made. For example, this method produced 3 to 12 nm Co nanoparticles in anhydrous DCB solutions.

SiNWs were made in a high-temperature furnace from nanoparticles deposited on silicon wafers. The growth conditions of these SiNWs were similar to those described elsewhere.[42] In brief, silicon wafers were immersed in cobalt nanoparticle solutions for up to 15 min while under sonication. The wafers were then removed from the solution, either rinsed with DI water or directly dried with Ar. The processed wafers were then placed in the center of a quartz tube in the high-temperature furnace. The quartz tube was sealed, and gases (Ar and H_2) were fed into the tube. The pressure was maintained at 0.5−1 psi above ambient pressure. The temperature was then increased to the growth temperature, which was 1100 °C. The maximum rate of temperature ramping was limited by the furnace controller, which was 25 °C/min. SiNWs produced this way were predominantly straight.

The SiNWs were first treated with aminopropyl-trimethoxy silane (APTMS). Typically, 10 mg SiNWs or small pieces of Si wafer with SiNWs grown on the surface were dispersed in 20 mL of ethanol. The solution was sonicated, and 0.05 mL of APTMS was added to the solution. The mixture was refluxed for 2 h at 120 °C and was then centrifuged and washed with ethanol three times.

To test whether APTMS was on the surface of SiNWs, ∼0.5 g of ninhydrin was added to 8 mL of APTMS functionalized SiNWs dispersed in an HPLC-grade ethanol−water mixture. After a brief period of sonication, the color of the mixture turned pale yellow. The mixture was heated on a hot plate, and when it was boiling, the color of the mixture gradually turned purple if there were amine groups on the surface.

For the patterned growth of SiNWs, letters were written on small silicon wafers using a syringe filled with a DCB solution of Co nanoparticles. The wafers were then placed in the furnace for nanowire growth. The samples were then inspected with scanning electron microscopy (SEM) and later functionalized with APTMS for ninhydrin testing.

Three types of gold nanoparticles were synthesized for the functionalization of SiNWs. Detailed information is given in Supporting Information. The first kind was gold nanoparticles covered with citrate ligands.[43,44] A second type of gold nanoparticle was made using mercaptoundecanoic acid (MUA) as a surfactant.[45] These nanoparticles were also used for making peptide bonds between the gold nanoparticles and APTMS-modified SiNWs. The third kind of gold nanoparticle was made with the weaker surfactant tetrakis-hydroxymethyl-phosphonium chloride (THPC).[46]

The assembly of gold nanoparticles on the surface of SiNWs was attempted using three approaches. Water solvent was used here unless specifically noted. The first method was to link citrate-covered gold nanoparticles to APTMS-functionalized SiNWs via electrostatic interactions at different pH values.[7] Typically, 5 mL of such a gold nanoparticle solution was mixed with 5 mL of APTMS-functionalized SiNWs. After keeping the mixtures at 4 °C for 10 h, a red precipitate appeared, indicating that gold nanoparticles were conjugated to the surface of SiNWs. The mixture was then centrifuged and washed with citrate acid (pH 6.4) three times and redispersed in citrate acid. Several drops of the solution were deposited on a copper transmission electron microscopy (TEM) grid for characterization. Because the interaction between citrate and APTMS was electrostatic, the pH value of the solution affected the formation of the nanoparticle−nanowire heterostructure. We prepared these heterostructures under either acidic or basic conditions using a 0.15 M citrate acid (pH 4.0) or 0.1 M NaOH (pH 10.4) solution. Under acidic conditions, a red precipitate appeared at once, and it was centrifuged and washed with citrate acid (pH 4.0) three times. However, very little red precipitate was observed after 24 h under basic conditions. The products were centrifuged and washed with NaOH solution (pH 10.4) three times. About 10% of the original product was recovered.

The second method was via the formation of peptide bonds.[47] In this method, 2 mL of MUA-functionalized gold nanoparticle solution, 10 mg of APTMS-functionalized SiNWs, 30 mg of *N*-(3-dimethyl-aminopropyl)-*N*′-ethylcarbodiimide hydrochloride (EDC), and 30 mg of *N*-hydroxysuccinimide (NHS) were mixed in 50 mL of phosphate buffer saline (PBS) (pH 7.5). The system was rapidly stirred for 8 h at 50 °C, and a red precipitate appeared. The precipitate was centrifuged and washed with PBS (pH 7.5) three times to remove free EDC, NHS, and water-soluble gold nanoparticles. The final product was dispersed in 20 mL of PBS. To verify the formation of the peptide bond, 5 mL of the solution was placed in two vials, with the pH value of one of the vials set to 2.3 and another one set to 11.5. The solutions were centrifuged after brief sonication. The coverage of gold nanoparticles did not change under either acidic or basic conditions. These results confirmed the formation of peptide bonds between gold nanoparticles and SiNWs.

To further reduce the repulsion between carboxylic terminating groups of the ligands on gold nanoparticles during surface coating,

(31) Law, M.; Greene, L.; Johnson, J.; Saykally, R.; Yang, P. *Nat. Mater.* **2005**, *4*, 455−459.
(32) Lapierre-Devlin, M.; Asher, C.; Taft, B.; Gasparac, R.; Roberts, M.; Kelley, S. *Nano Lett.* **2005**, *5*, 1051−1055.
(33) Ahn, Y.; Dunning, J.; Park, J. *Nano Lett.* **2005**, *5*, 1367−1370.
(34) Zhong, Z.; Fang, Y.; Lu, W.; Lieber, C. *Nano Lett.* **2005**, *5*, 1143−1146.
(35) Thelander, C.; Nilsson, H.; Jensen, L.; Samuelson, L. *Nano Lett.* **2005**, *5*, 635−638.
(36) Yu, D. P.; Hang, Q. L.; Ding, Y.; Zhang, H. Z.; Bai, Z. G.; Wang, J. J.; Zou, Y. H.; Qian, W.; Xiong, G. C.; Feng, S. Q. *Appl. Phys. Lett.* **1998**, *73*, 3076−3078.
(37) Ma, D.; Lee, S.; Shinar, J. *Appl. Phys. Lett.* **2005**, *87*, .
(38) Li, C.; Sun, X.; Wong, N.; Lee, C.; Lee, S.; Teo, B. *J. Phys. Chem. B* **2002**, *106*, 6980−6984.
(39) Sheu, J.; Chen, C.; Huang, P.; Hsu, M. *Microelectron. Eng.* **2005**, *78*−*79*, 294−299.
(40) Carter, J. D.; Cheng, G.; Guo, T. *J. Phys. Chem. B* **2004**, *108*, 6901−6904.
(41) Puntes, V. F.; Krishnan, K. M.; Alivisatos, A. P. *Science* **2001**, *291*, 2115−2117.
(42) Carter, J. D.; Qu, Y. R. P.; Hoang, L.; Masiel, D. J.; Guo, T. *Chem. Commun.* **2005**, 2274−2276.
(43) Frens, G. *Nat. Phys. Sci.* **1971**, *24*, 21.
(44) Brown, K.; Walter, D.; Natan, M. *Chem. Mater.* **2000**, *12*, 306−313.
(45) Hiramatsu, H.; Osterloh, F. E. *Langmuir* **2003**, *19*, 7003−7011.
(46) Duff, D.; Baiker, A.; Gameson, I.; Edwards, P. *Langmuir* **1993**, *9*, 2310−2317.
(47) Ravindran, S.; Chaudhary, S.; Colburn, B.; Ozkan, M.; Ozkan, C. *Nano Lett.* **2003**, *3*, 447−453.

a third kind of gold colloidal nanoparticles with THPC-capping ligands was used.[48] Specifically, 5 mL of an APTMS-functionalized SiNW solution (1 mg/mL) in ethanol was put into a centrifuge tube. A pre-prepared gold colloid (5 mL) was added, and the centrifuge tube was shaken for 10 min and then allowed to rest for 2 h, giving rise to a brown precipitate. The product was centrifuged and washed with HPLC-grade water three times. The purified product was redispersed in 5 mL of HPLC-grade water. However, 100% coverage was still not achieved.

One hundred percent gold coverage or gold tubular nanoshells on SiNW templates were prepared from several gold precursor solutions using a regrowth method. Typically, 25 mg of potassium carbonate was dissolved in 100 mL of HPLC grade water. After 10 min, 1.5 mL of a 1% $HAuCl_4$ aqueous solution was added to the K_2CO_3 aqueous solution. The color of the mixture changed slowly from light yellow to colorless over 30 min. The $HAuCl_4/K_2CO_3$ solution (10 mL) was aged for 1 day and placed into a 50 mL flask.[48] The solution was rapidly stirred while 50 μL of 29% formaldehyde was injected. A pre-prepared THPC-capped gold nanoparticle−APTMS-functionalized SiNWs mixture (100 μL) was then slowly injected into the mixture. The color of the mixture turned light blue after 2−5 min, and a black precipitate appeared quickly. The product was centrifuged and washed with HPLC-grade water two times. The washed product was redispersed in 5 mL of HPLC-grade water. The amount of $HAuCl_4/K_2CO_3$ was adjusted to maximize the coverage. If needed, these nanotube−nanowire heterostructures were etched in 5% HF solutions for 10 h to remove the silica core.

Similarly, Ag tubular nanoshells were prepared. $AgNO_3$ aqueous solutions of three concentrations (0.25, 0.6, and 1.0 mM) were used. Each of these freshly prepared $AgNO_3$ aqueous solutions (10 mL) was mixed with the same THPC-capped gold nanoparticle seeds on SiNWs. While each mixture was rapidly stirred, 60 μL of 29% formaldehyde was injected into the mixture. Then 50 μL of 3 M $NH_3 \cdot H_2O$ was added to the solution. The solution became opaque, and a black precipitate appeared. Stirring was continued for 15 min.

TEM (Philips CM-12 and CM-300) was used to inspect the samples. The CM-300 was located at the National Center for Electron Microscopy (NCEM), and it was capable of obtaining high-resolution images. Samples were dropped onto TEM grids (Formvar, Ted Pella) and air dried. An SEM (FEI XL-30 SFEG) was also used to examine the samples (acceleration voltage 5 kV). The resolution was approximately ∼2 nm. Samples were prepared on different substrates, including Si wafers and alumina substrates.

^{29}Si nuclear magnetic resonance (NMR) spectroscopy was used to detect the chemical environment of Si atoms in silica nanowires. ^{29}Si single-pulse (SP) magic angle spin (MAS) and cross polarization (CP) MAS NMR experiments were performed on a Bruker Avance 500 spectrometer equipped with an 11.75 T magnet. The ^{29}Si resonance frequency was 99.35 MHz. A Bruker 7 mm CPMAS solid NMR probe and 7 mm zirconia rotor were used at a spinning rate of 5 kHz. The ^{29}Si and ^{1}H 90° pulse width was 6 μs. The contact time was 5 ms, and the pulse recycle delay was 5 s for CPMAS and 300 s for direct polarization experiments. The chemical shifts were externally referenced to tetramethylsilane (TMS).

The photoluminescence measurements were performed with a fluorometer (Fluromax-P, Jobin Yvon). A more sensitive setup was used in which backscattered light was collected with a microscope interfaced with three lasers lines at 532, 632, and 780 nm. The setup was similar to that of a microscope described elsewhere.[49] SiNW samples directly removed from the surface were examined.

Results

Figure 1 shows the results of the bulk synthesis of SiNWs at 1100 °C. Figure 1A is an SEM image of these nanowires. They are generally straight with an average persistence length over 1 μm. Figure 1B shows a photograph of a bulk SiNW sample grown on a Si wafer for 12 h. The thickness of the SiNW film

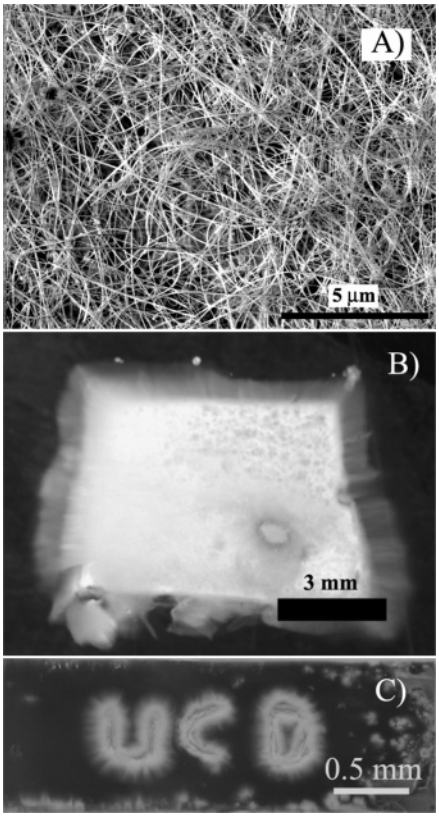

Figure 1. Silica nanowires. (A) SEM image. (B) Photograph of a sample after 12 h of growth. A 1.5-mm-thick layer of SiNWs is clearly seen. (C) Area-selected growth of SiNWs.

was ∼1.5 mm. Figure 1C shows the patterned growth of SiNW films from inscribed letters written with the syringe pen of a Co nanoparticle solution. This result showed that high-yield growth of SiNWs (white material in 1C) required the presence of Co nanoparticles because the areas without Co nanoparticles had almost no SiNWs.

Figure 2 shows the detailed structures of SiNWs. They were generally very long, and it was difficult to measure their length because the ends disappeared in the bulk. Figure 2A shows a histogram of the diameters of these nanowires. SiNWs as thin as 5 nm were observed, although the nominal diameter was 43 nm. Figure 2B and C shows HRTEM images of a SiNW, which shows that this nanowire has an amorphous core. On the basis of the geometry of SiNWs, the surface area was estimated to be 40 m^2/g. This value is higher than that of normal silica gels (1−10 m^2/g) but is lower than that of nanoparticle aerosols (100 m^2/g).

The NMR results are shown in Figure 3. Both SP and CP results are shown. The first indication of these results was that there were no detectable amounts of crystalline Si in the sample, which should result in a narrow peak at −81 ppm. Si atoms in an oxygen environment generally yield four peaks, denoted Q1 ($Si(OH)_3O$), Q2 ($Si(OH)_2O_2$), Q3 ($Si(OH)O_3$), and Q4 (SiO_4).[50,51] These peaks were between −80 and −110 ppm. Regular SP scans showed only one peak, which was the Q4 peak that corresponds to the SiO_2 network with a Si atom connected to four bridging oxygen atoms. Using the CP technique, it was possible to detect surface Si atoms more preferentially, which may have one or more hydrogen-terminating oxygen atoms

(48) Pham, T.; Jackson, J.; Halas, N.; Lee, T. *Langmuir* **2002**, *18*, 4915−4920.
(49) Porter, R.; Shan, F.; Guo, T. *Rev. Sci. Instrum.* **2005**, *76*, .
(50) Nishikawa, H.; Shiroyama, T.; Nakamura, R.; Ohki, Y.; Nagasawa, K.; Hama, Y. *Phys. Rev. B* **1992**, *45*, 586−591.
(51) Gotza, M.; Dutoit, M.; Ilegems, M. *J. Vac. Sci. Technol., B* **1998**, *16*, 582−588.

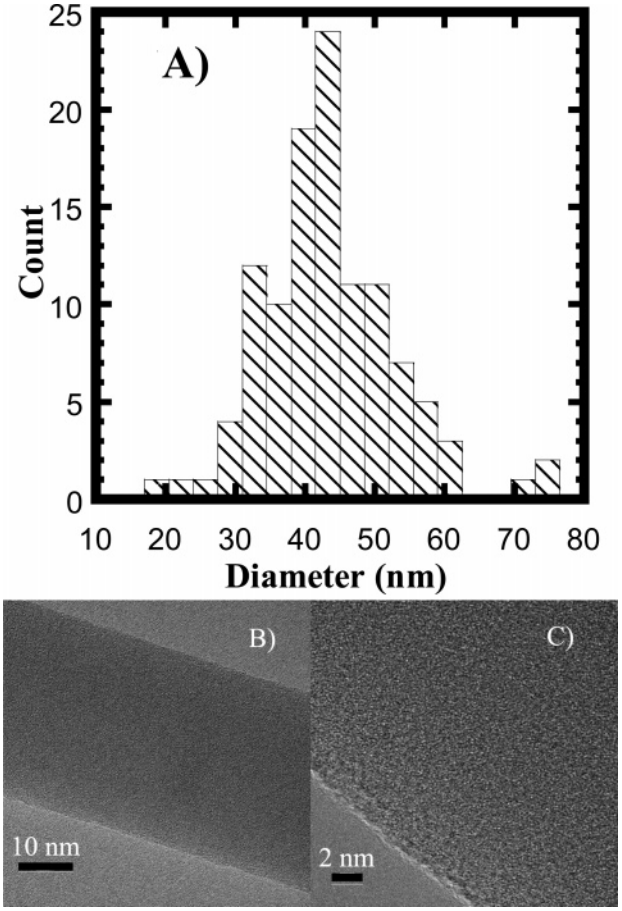

Figure 2. Morphologies (diameter and structures) of SiNWs. (A) The average diameter is 43 ± 4 nm, and (B and C) all SiNWs are amorphous on the basis of high-resolution TEM images.

connected to the Si atoms. In Figure 3B, three closely spaced peaks are shown, corresponding to Q2, Q3, and Q4 peaks. Q3 was the most intense peak, indicating that the majority of the surface Si atoms were in the configuration of $Si(OH)O_3$.

Photoluminescence (PL) results are shown in Figure 4A. Only one peak at 380 nm was visible with 240−260 nm excitation. This peak corresponds to the 3.1 eV peak in the normal PL spectrum of SiO_2 with oxygen vacancies, possibly caused by the 2-fold-coordinated silicon lone-pair centers (O−•Si•−O).[50] However, a second PL peak at 650 nm, which corresponds to the nonbridging oxygen hole centers (≡Si−O•), was visible when laser-based PL measurements were performed. Figure 4B shows the results with 532, 632, and 780 nm excitation light. Because the PL peak was located at 650 nm, the 532 nm excitation produced the strongest PL. Under 632 nm excitation, the PL was weaker, as shown in Figure 4B. The PL signal detected at longer wavelength with 780 nm light excitation was much weaker compared to that from 532 (400×) and 632 nm (6×) excitation.

SiNWs appeared to be soluble in water. However, these nanowires eventually precipitated after a few hours because of their large sizes. When dispersed in water and quickly filtered with 50 nm filter papers, 70% of SiNWs were recovered by redissolving the filter papers in water and sonicating for 10 min. The results of testing APTMS-functionalized SiNWs are shown in Figure 5. When functionalized with APTMS, SiNWs were more soluble in water. Compared to pure SiNWs, these nanowires scattered less light when they were dispersed in water. Figure 5A shows the results of scattering 650 nm light from a laser pointer. As shown, the functionalized SiNWs (left) were much

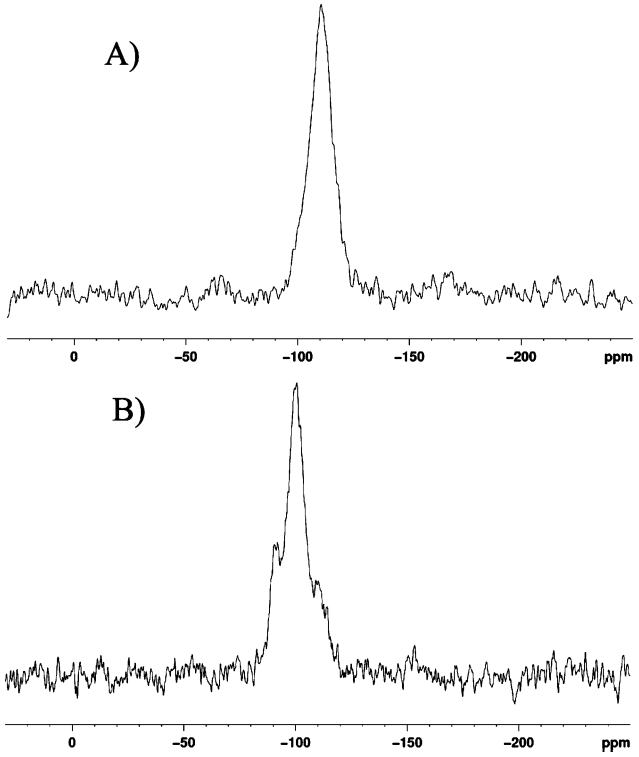

Figure 3. (A) Single pulse ^{29}Si and (B) $^{1}H-^{29}Si$ cross-polarization NMR results. The single peak in A corresponds to Q4 peak in the SiO_4 bonding structure. Three peaks are seen in B, corresponding to Q2 (at −90 ppm), Q3 (at −100 ppm), and Q4 (at −110 ppm).

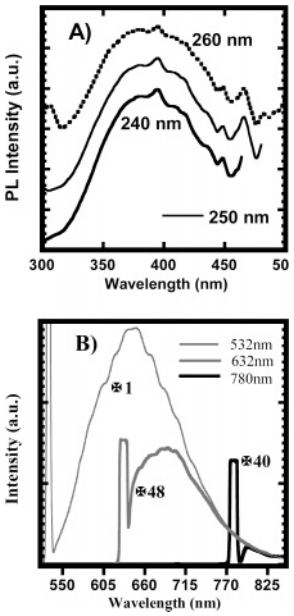

Figure 4. Photoluminescence (PL) results of SiNWs. (A) PL in the 300−500 nm range with 240−260 nm excitation. Only one broad peak was observed at ∼380 nm. (B) PL in the 500−850 nm range at three different excitation wavelengths: 532, 632, and 780 nm. The 632 and 780 nm induced PL profiles were normalized to that of 532 nm excitation (the most intense one).

less scattering. This can be attributed to the fact that the average particle size of the aggregates of SiNWs was smaller for APTMS-functionalized SiNWs because they were individual nanowires. It was also possible that APTMS-functionalized SiNWs were more soluble in water, thus lowering the refractive index change at the interface of water and SiNWs. As mentioned earlier, APTMS-covered SiNWs can be detected with ninhydrin. In Figure

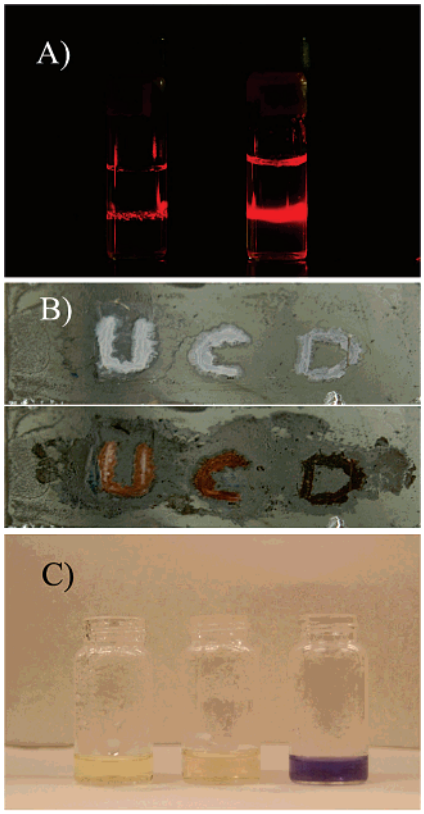

Figure 5. Functionalization and detection of SiNWs. (A) APTMS-functionalized SiNWs were more readily dissolved and dispersed in water. As a result, the SiNW solution (left vial in A) scattered less than free-standing SiNW aggregates (right vial in A) under the illumination of a laser beam. (B and C) Ninhydrin detection of the amine group in APTMS was used. Upon reaction with ninhydrin, SiNWs turned red, as shown by the letter "D" in panel B and the right vial in panel C.

5B, the letters of SiNWs were immersed in ninhydrin solution. Upon heating, the letters turned pink, indicating that there was amine on the surface. A darker color represented a higher-density amine. This result was also repeated with a SiNWs aqueous solution, as shown in Figure 5C. The bottle on the right shows that the color of APTMS-functionalized SiNWs turned purple/pink when heated in the presence of ninhydrin. The bottle in the middle in Figure 5C contained pure SiNWs without APTMS. Upon adding ninhydrin, the solution remained colorless. The left bottle in Figure 5C shows a solution of functionalized SiNWs in water.

To demonstrate that SiNWs can be used as templates to make other nanostructures, we investigated whether it was possible to grow gold tubular nanoshells directly on the surfaces of these SiNWs. As will be shown, it was difficult to produce gold tubular shells through a one-step process. In the following discussion, the results of a two-step procedure involving first decorating SiNWs with gold nanoparticle seeds followed by adding metal precursors to restart the growth processes are given.

Figure 6 shows the results of gold nanoparticle syntheses. Figure 6A shows the results of citrate-capped gold nanoparticles. The size distribution was 3.1 ± 0.85 nm. Figure 6B shows a TEM image of MUA-covered gold nanoparticles. The average size was 6.1 ± 1.1 nm. Figure 6C shows a TEM image of THPC-terminated gold nanoparticles. The average size was 2.5 ± 0.68 nm. These nanoparticles were used to make gold and silver tubular nanoshells on SiNWs.

Figure 7A−C shows the results of linking citrate-capped gold nanoparticles to APTMS-functionalized SiNWs via electrostatic

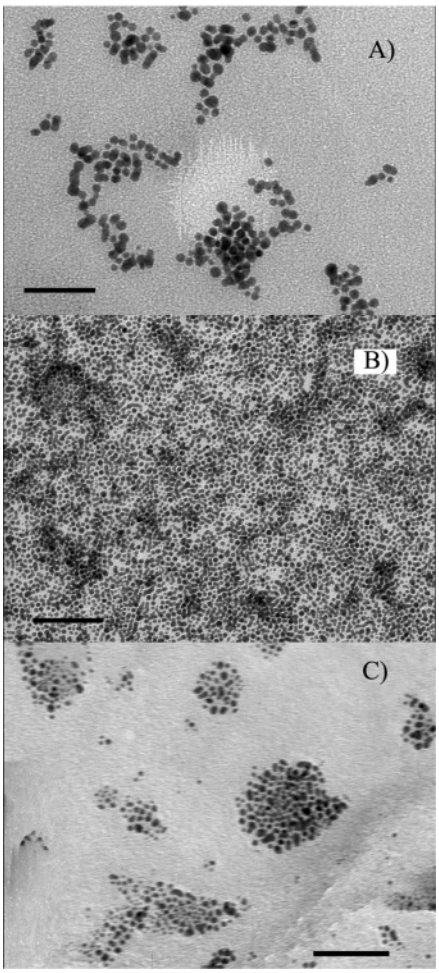

Figure 6. Three types of gold nanoparticles used in the functionalization of SiNWs. (A) Citrate, (B) MUA, and (C) THPC were the surfactants on these nanoparticles. The average diameters were between 2 and 5 nm. The scale bars in A and C are 50 nm, and that in B is 100 nm.

interactions at different pH values. The coverage of gold nanoparticles on SiNWs depended on the pH of the solution. Figure 7A shows a TEM image of the nanoparticle−nanowire heterostructure at pH 6.4. It is obvious that individual nanoparticles were on the surface of silica nanowires. The surface coverage of the nanowires was ~25%, limited by the electrostatic repulsion between these negatively charged gold nanoparticles in pH 6.4 solution. Figure 7B shows the TEM picture of the products at a more basic condition (pH 10.4). The coverage was lower. Figure 7C is a TEM picture of the heterostructure at pH 4.0. The surface coverage was higher, although nonuniform. There were also aggregates of nanoparticles, and no continuous tubes were formed. This can be explained because at lower pH values the amino groups on the surface of the SiNWs were more positively charged, resulting in a higher electrostatic force between the negatively charged citrate-capped gold nanoparticles and positively charged amine groups on SiNWs, thus resulting in a higher coverage. In contrast, higher pH values induced a lower coverage because NH_2 was less positively charged.

Another way to decorate gold nanoparticles on SiNWs was to form peptide bonds between the amine groups on SiNWs and carboxylic groups on the gold nanoparticles. Figure 7D shows the result, and again only moderate coverage was achieved. These heterostructures were not easily affected by the pH of the solutions. For example, solutions with pH from 2 to 11 were used to wash the product, and the coverage remained the same.

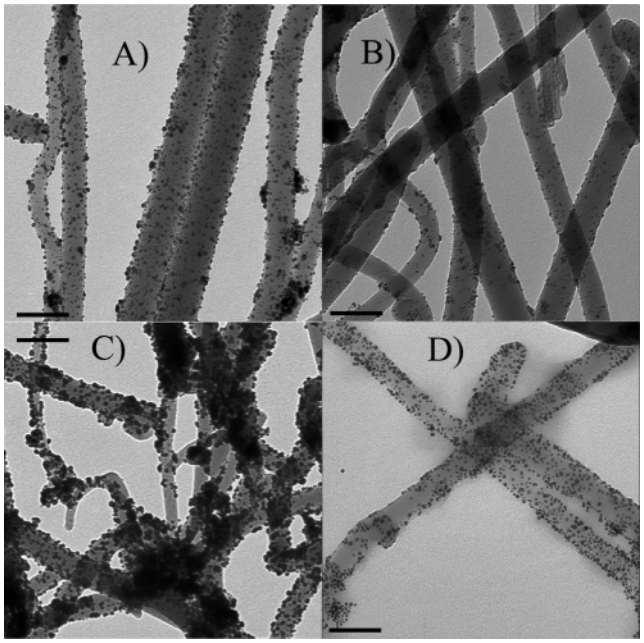

Figure 7. Functionalization of SiNWs with gold nanoparticles at three different pH values—(A) pH 6.4, (B) pH 10.4, and (C) (pH 4.0)—and (D) MUA covalently linked gold nanoparticles to SiNWs. The scale bar is 200 nm in all panels.

As shown in Figure 7, the coverage was far below 100% using these methods. To overcome this problem, seeded growth was used. In this approach, THPC-capped gold nanoparticles were conjugated to the surface of APTMS-functionalized SiNWs, as shown in Figure 8A. Gold precursors such as an aged $HAuCl_4$/K_2CO_3 solution were added to restart the growth. Figure 8B−D shows the results of increasingly larger volumes of gold precursors used for the seeded growth. As shown, SiNWs in Figure 8B had approximately 50% coverage when 2.5 mL of precursors was used. The addition of 5 mL of precursors resulted in a higher coverage, as shown in Figure 8C. Maximum coverage was achieved with the addition of 10 mL of precursors. The result is shown in Figure 8D. These results clearly illustrate the evolution of the formation of tubular nanoshells on the surface of SiNW templates. In some cases, the end sections of SiNWs were left uncoated, which strongly suggested that the gold was in the form of tubular nanoshells wrapping around the SiNWs. Two examples are given in Figure 9A and C. Figure 9B shows one such gold nanotube after HF etching. The silica nanowire core disappeared, but the nanotube remained intact.

Optical measurements were used to determine whether these tubular nanoshells were indeed made of gold metal or were simply aggregates of small gold nanoparticles. The optical absorption results are shown in Figure 10. The absorption data of preformed gold nanoparticles themselves and that of gold nanoparticles linked to the surface of SiNWs are shown in Figure 10A, and that of the gold tubular nanoshells is shown in Figure 10B. To record the absorption data, these tubular nanoshells must be made more soluble in water. In this case, 3-mercaptopropionic acid (MPA) ligands were used to funcationalize the surface of the gold tubular nanoshells similar to that of MUA on gold nanoparticles described earlier. After functionalization, gold tubular nanoshells remained soluble in water for hours. As shown in Figure 10B, the absorption peak was red shifted from 530 to 630 nm. It has been shown that ∼100 nm gold nanoparticles, which are almost gold bulk, exhibit an absorption peak at 630 nm.[52] Because the overall diameter of the tubular nanoshells was ∼100 nm, this result indicated that the gold tubular nanoshells

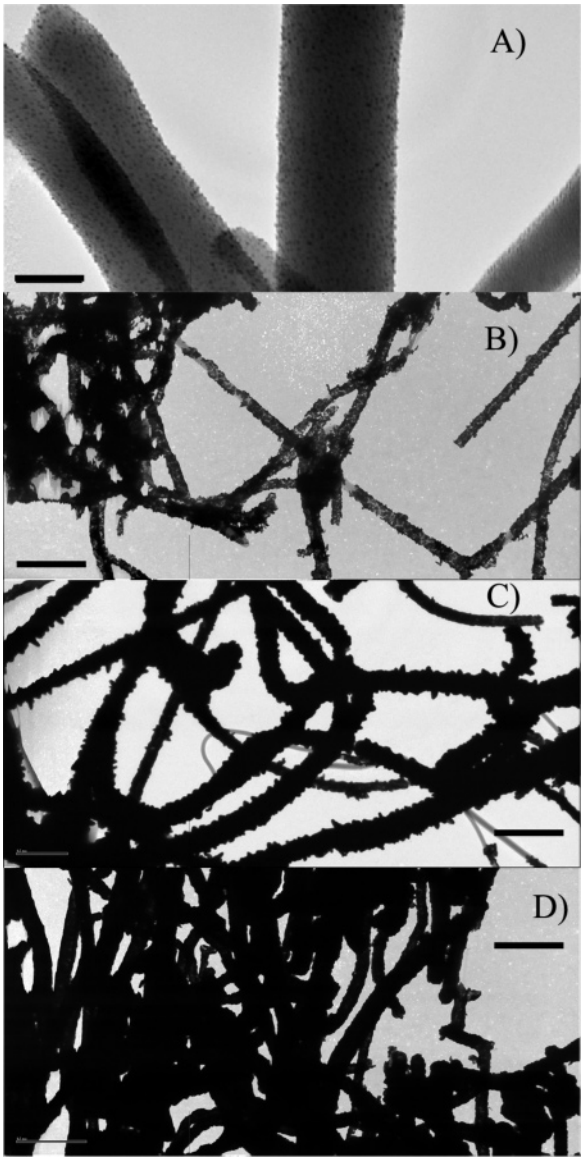

Figure 8. (A) Results of regrowth to form gold tubular nanoshells on SiNWs with the THPC-capped gold nanoparticle seeds on SiNWs. (B) 2.5, (C) 7.5, and (D) 10 mL of a $HAuCl_4$/K_2CO_3 solution were used with a fixed amount of SiNWs (10 mg) to form these tubes. Larger amounts of gold led to higher gold coverage. The scale bars are (A) 50 and (B−D) 500 nm.

synthesized here were indeed gold metal, not aggregates of small gold nanoparticles.

The seeded growth was also applied to Ag to form silver tubular nanoshells. In this case, THPC-capped gold nanoparticles were used as the seeds. Again, at low silver concentration of 0.25 mM, SiNWs were not fully covered with Ag (shown in Figure 11A), similar to those shown in Figures 7D and 8A. Upon increasing the concentration of Ag salts, the nanowires became more fully covered with Ag to form Ag tubular nanoshells, as shown in Figure 11B (0.6 mM) and C (1 mM). Again, these pictures clearly show the evolution of the formation of silver tubular nanoshells.

The results shown above indicated that gold and silver tubular nanoshells were made as metal overlayers coating the entire SiNWs. It is also possible to etch away the SiO_2 core and produce Au and Ag tubular nanoshells without SiO_2 in the middle. SEM/EDX results before and after etching with HF showed that the

(52) Link, S.; El-Sayed, M. *J. Phys. Chem. B* **1999**, *103*, 4212−4217.

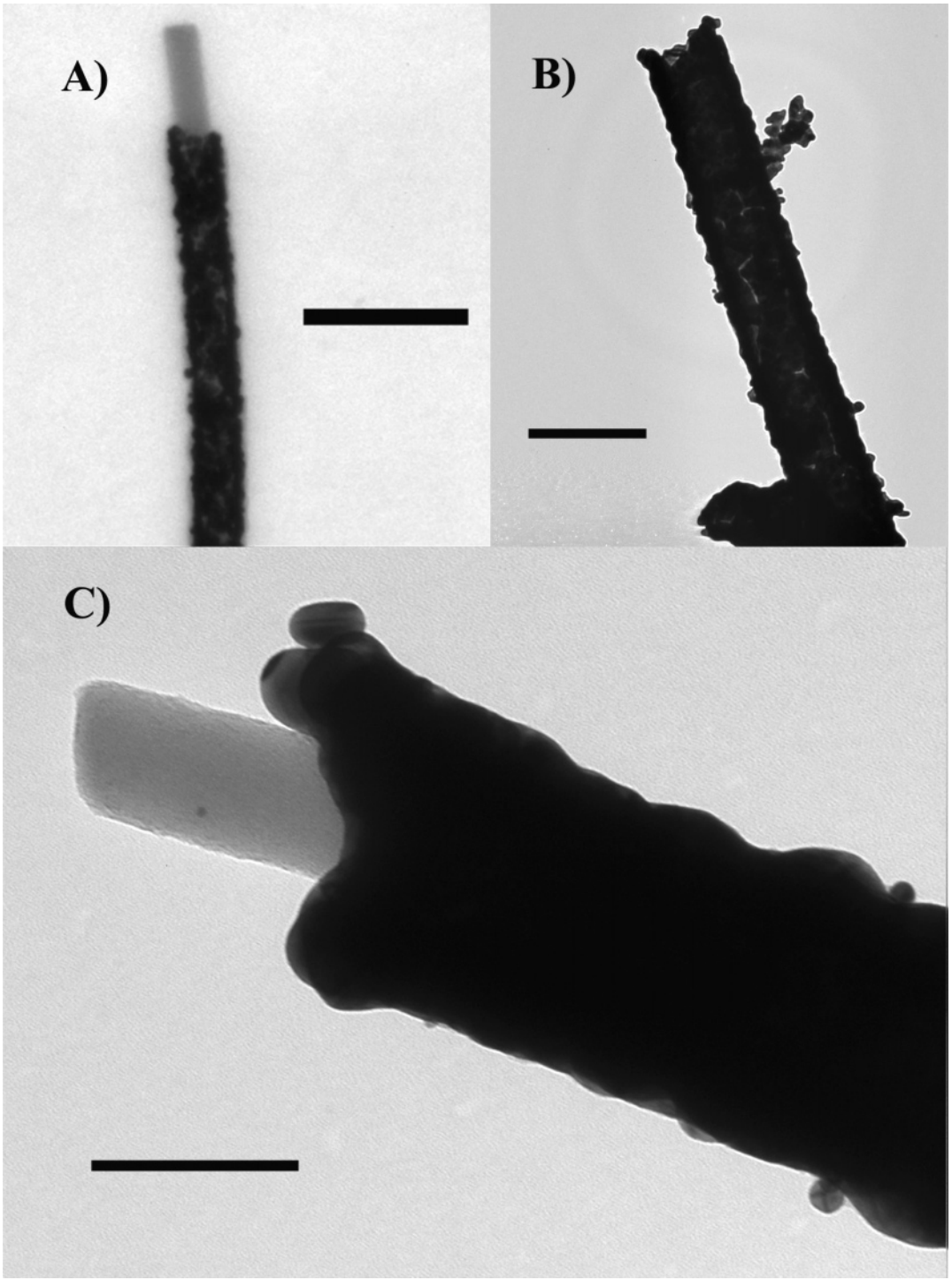

Figure 9. (A and C) TEM images of SiNWs sticking out of gold tubular nanoshells and (B) that of an etched nanotube. Short SiNWs were visible at the end of gold tubular nanoshells in A and C. The scale bars are (A) 500, (B) 200, and (C) 100 nm.

content of Si was reduced by a factor of 5 after 12 h of etching. For SiNWs with less than 100% coverage of Au tubular nanoshells, SiO_2 was readily etched away through holes on patchy tubular nanoshells (Figures 8A and 11A).

Discussion

The result of less than 100% coverage of gold nanoparticles on SiNWs using several one-step functionalization approaches can be explained by the repulsion between the charged ligands on these gold nanoparticles. Although amine groups of APTMS on SiNWs attracted nanoparticles covered with strongly negatively charged groups such as citrate through electrostatic interactions, eventually it became too difficult for these gold nanoparticles to move close to the surface of SiNWs, repelled by the charged gold nanoparticles already on the surface of SiNWs. Therefore, only weakly negatively charged groups such as THPC allowed a high-density, uniform coverage of gold nanoparticles on the surface. However, no continuous coverage of gold metal was achieved even with THPC-capped gold nanoparticles, and gold precursors had to be used. It was also possible that the size of gold nanoparticles was important: smaller nanoparticles favored higher coverage because of the smaller number of ligands per nanoparticle.

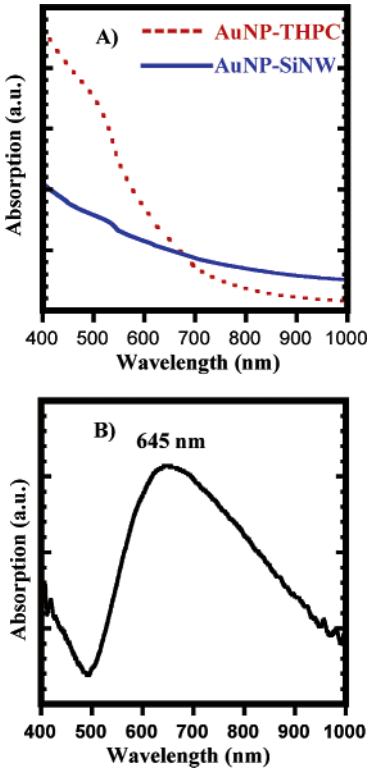

Figure 10. UV−vis absorption of (A) THPC-capped gold nanoparticles and gold nanoparticle-functionalized SiNWs and (B) MPA-functionalized gold tubular nanoshells. MPA functionalization was necessary to make gold tubular nanoshells more soluble in water. The main absorption peak shifted from 530 nm in A for the nanoparticles to 645 nm for tubular nanoshells in B.

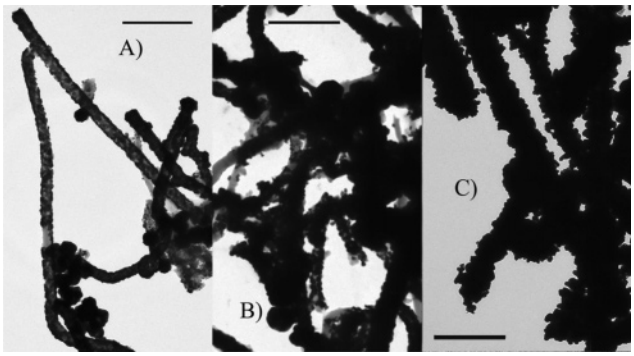

Figure 11. Results of regrowth to form silver tubular nanoshells on SiNWs. Ten milliliters of (A) 0.25, (B) 0.6, and (C) 1.0 mM $AgNO_3$ (aq) solutions were used with a fixed amount of SiNWs (10 mg) to form these tubular nanoshells. Larger amounts of silver led to higher coverage. The scale bars are 500 nm.

The use of THPC also reduced the repulsion between gold precursors and the gold nanoparticle seeds. As a result, gold precursors could be more easily added to the surface of SiNWs. The same mechanisms may be true for silver addition to the surface, though the seeds were still THPC-capped gold nanoparticles. Another possible explanation for the low coverage of gold nanoparticles on SiNWs could be attributed to low APTMS coverage on SiNWs, although this was unlikely because of the high coverage of THPC-capped gold nanoparticles.

The regrowth step was important for making continuous gold or silver tubular nanoshells on SiNW templates. It provided another parameter with which one can adjust the growth conditions. For example, when nonaged stocking solutions were used, the formation of tubular nanoshells proceeded either too quickly or too slowly, depending on the choice of the reducing agent. As a result, either gold nanoparticles formed in solution but not on the gold nanoparticle seeds on the surface of SiNWs when strong reducing agents such as $NaBH_4$ were used or very little gold was reduced when weak reducing agents such as formaldehyde were used. To avoid these two problems, the $HAuCl_4/K_2CO_3$ solution was aged for a day. In this case, the gold ions in the solution were converted from $AuCl_4^-$ to $Au(OH)_3$, which was then reduced by formaldehyde.[53] This turned out to be critical to the addition of gold atoms to gold nanoparticle seeds that were already on the SiNWs. This result has also been observed elsewhere.[48]

As shown in the PL measurements, the intensity of PL from these SiNWs was relatively weak. This indicates that the density of oxygen vacancies was low. This also supported the notion that no crystalline Si core existed in SiNWs, which normally helps to create oxygen vacancies at the interface of the crystalline core and the amorphous SiO_2 outer layer. Because we did not control the vacuum of the synthetic apparatus and relied on the purge gases at a pressure slightly above ambient to keep away the oxygen, SiNWs could be crystalline as synthesized and subsequently oxidized upon exposure to the air or trace oxygen in the reaction chamber at 1100 °C. Future work will be needed to determine and control the source of oxygen.

As shown in Figure 4, there was still a significant amount of light scattered even with the 780 nm excitation. We determined that this scattered light could come only from PL because the wavelength shift of Rayleigh scattering could not extend that far away from the excitation wavelength. Rayleigh scattering can shift the wavelength only by a few nanometers from the original excitation wavelength. The weak PL may be caused by various defects or oxygen vacancies in SiNWs, with its emission centered around 650 nm. These nanowires may offer a good opportunity to study light scattering because they are highly anisotropic: Rayleigh scattering would occur preferentially along the cross section whereas Mie scattering would occur along the length dimension.

Conclusions

We made SiO_2 nanowires and manipulated them as templates to make gold and silver tubular nanoshells by first decorating the nanowires with small gold nanoparticle seeds and then initiating a regrowth process in gold or silver stock solutions. Compared to this method, it was almost impossible to grow tubular nanoshells directly through any one-step processes. This method should be applicable to synthesizing other metal tubular nanoshells on SiNW templates.

Acknowledgment. We are grateful for financial support from the National Science Foundation (scattering measurements supported by CHE 0135132). This work is partially supported by the UC Campus − National Laboratory Exchange Program (CLE). We thank Dr. Ping for her assistance with the NMR experiments. We thank Dr. C. Song at the National Center for Electron Microscopy (NCEM) for his assistance. NCEM is a facility supported by the Department of Energy. J.D.C. thanks Tyco for the Tyco Fellowship for Research in Electronic Materials.

Supporting Information Available: Experimental details of preparing three types of gold nanoparticles. This material is available free of charge via the Internet at http://pubs.acs.org.

LA060359M

(53) Weiser, H. B. *Inorganic Colloid Chemistry*; John Wiley & Sons: New York, 1933; Vol. 1, p 389.